Medicinal Chemistry Research (2023) 32:342–354
https://doi.org/10.1007/s00044-022-03009-3

MEDICINAL CHEMISTRY RESEARCH

ORIGINAL RESEARCH

Synthesis and bioactivity evaluation of pachymic acid derivatives as potential cytotoxic agents

Hezhen Wang[1] · Xun Sun[1] · Chunyong Wei[1] · Jing Wang[1] · Yingshu Xu[1] · Guohui Bai[2] · Qizheng Yao[3] · Lei Zhang[1]

Received: 2 September 2022 / Accepted: 16 December 2022 / Published online: 29 December 2022

Abstract

Pachymic acid, a well-known natural lanostane-type triterpenoid, exhibits various pharmacological properties. In this study, 18 derivatives of pachymic acid were synthesized by modifying their molecular structures and evaluated for their anticancer activity against two human cancer cell lines using the CCK-8 assay. Structure-activity relationship studies according to the in vitro cytotoxicity unexpectedly found one promising derivative **A17** (namely tumulosic acid, also found in *Poria cocos*), which had stronger anti-proliferative activity than the positive drug cisplatin against HepG2 and HSC-2 cell lines with IC_{50} values of 7.36 ± 0.98 and 2.50 ± 0.15 μM, respectively. Further pharmacological analysis demonstrated that **A17** induced HSC-2 cell cycle arrest at the S phase, cell apoptosis, and autophagy. Western blotting confirmed the regulatory effects of **A17** on cell cycle arrest-, apoptosis-, and autophagy-related proteins expression. In addition, **A17** regulated the AKT and AMPK pathways in HSC-2 cells. These results demonstrated that **A17** possesses great potential as an anticancer agent.

Graphical Abstract

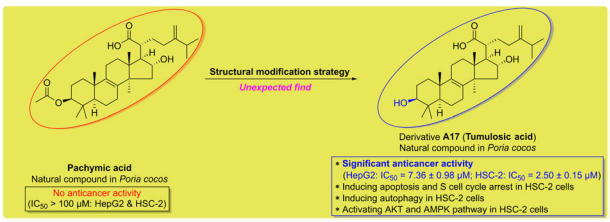

Keywords Pachymic acid · Structural modification · Anticancer activity · Tumulosic acid · Structure-activity relationship

Supplementary information The online version contains supplementary material available at https://doi.org/10.1007/s00044-022-03009-3.

✉ Yingshu Xu
xuyingshu1976@126.com

✉ Guohui Bai
baiguohui1228@126.com

✉ Lei Zhang
lzhang@zmu.edu.cn

[1] Key Laboratory of Biocatalysis & Chiral Drug Synthesis of Guizhou Province, Key Laboratory of Basic Pharmacology of Ministry of Education, School of Pharmacy, Zunyi Medical University, 563000 Zunyi, China

[2] Key Laboratory of Oral Disease Research, School of Stomatology, Zunyi Medical University, 563000 Zunyi, China

[3] Department of Medicinal Chemistry, School of Pharmacy, China Pharmaceutical University, 210009 Nanjing, China

Introduction

To date, cancer remains a global problem to human life and health [1]. Cancer is considered the leading cause of death worldwide. By 2030, 15 million deaths due to cancer have been estimated by the World Health Organization [2]. Although extensive efforts have been made over the last 20 years in cancer therapy, such as conventional medications, targeted treatments and combination therapies, the methods for high-grade and metastatic malignancies remain limited [3]. In pharmaceutical research, there is an urgent need to search for novel, effective, and safe chemotherapeutic drugs for cancer treatment [4].

Pachymic acid (PA, Fig. 1) is an important natural lanostane-type triterpenoid isolated from the wood-rotting fungus *Poria cocos* [5]. The sclerotium of *Poria cocos*, known as fu-ling or hoelen, has been widely used in various traditional Chinese medicines and health foods for hundreds of years [6, 7]. Several studies have shown that PA has significant biological activities, such as anticancer, anti-inflammatory, antibacterial, sedative-hypnotic, antihyperglycemic, and anti-ischemia/reperfusion effects [8–12]. Among these, the cytotoxic effects of PA in vitro and in vivo have attracted significant attention. PA has been shown to inhibit various cancer cells [13–18], including leukemia and cancers of the prostate, bladder, gastric, colon, and breast. In addition, PA also showed significant anticancer activities in animal models [19–21] by inhibiting the growth of NCI-H23, SGC-7901, and MIA PaCa-2 xenograft tumors. In a review of the pharmacological profiles and therapeutic applications of PA, we systematically summarized the anticancer potential of PA and its underlying molecular mechanisms in vitro and in vivo [22]. However, to date, there is limited knowledge regarding the modification on the structure of PA to improve its anticancer activity [23]. As part of our ongoing efforts to investigate natural products [24–28], 18 derivatives of PA were synthesized and evaluated for their in vitro cytotoxicity in two human cancer cell lines using the CCK-8 assay. In particular, the preliminary structure-activity relationship (SAR) and underlying molecular mechanisms were also examined.

Results and discussion

Chemistry

The synthetic routes of derivatives **A1**-**A10**, **A11**-**A16**, and **A17**-**A18** are shown in Schemes 1–3, respectively, with PA as the precursor. PA was esterified with alkyl bromides to give the corresponding 21-COOH ester products **A1**-**A6**. $NaBH_4$ has been reported to reduce esters [29]; therefore, we attempted to obtain diol **A7** using $NaBH_4$. Treatment of compound **A1** with $NaBH_4$ in alcohol under reflux conditions afforded compound **A7** via selective disintegration of the 3-acetate ester group, which might be related to the large steric hindrance of the 21-ester group. Diol **A7** was further oxidized in the presence of Dess-Martin periodinane to obtain diketone **A8**. Compound **A9** was generated by the oxidation of **A1** using Dess-Martin periodinane as the oxidizing agent. To synthesize compound **A10**, a hydrogen reduction reaction of benzyl ester in **A9** in the presence of Pd/C was conducted. To obtain the carbohydrate derivatives

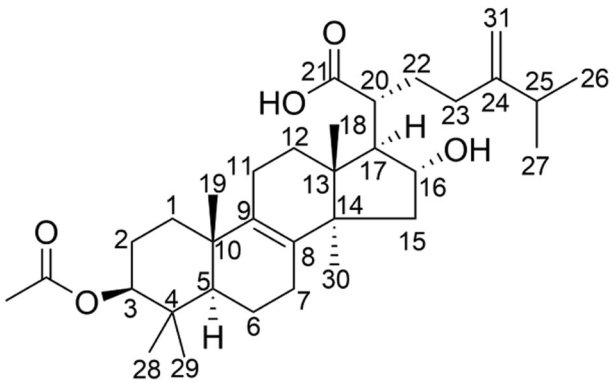

Fig. 1 The structure of pachymic acid

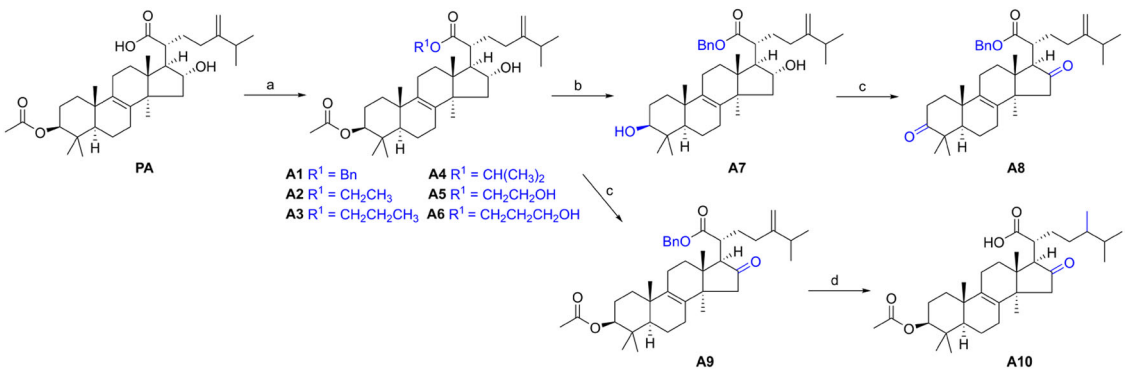

Scheme 1 Synthetic route of compounds **A1**-**A10**. Reagents and conditions: a R^1Br, K_2CO_3, DMF, room temperature; b $NaBH_4$, EtOH, reflux; c Dess-Martin periodinane, DCM, room temperature; d H_2, Pd/C, MeOH, room temperature

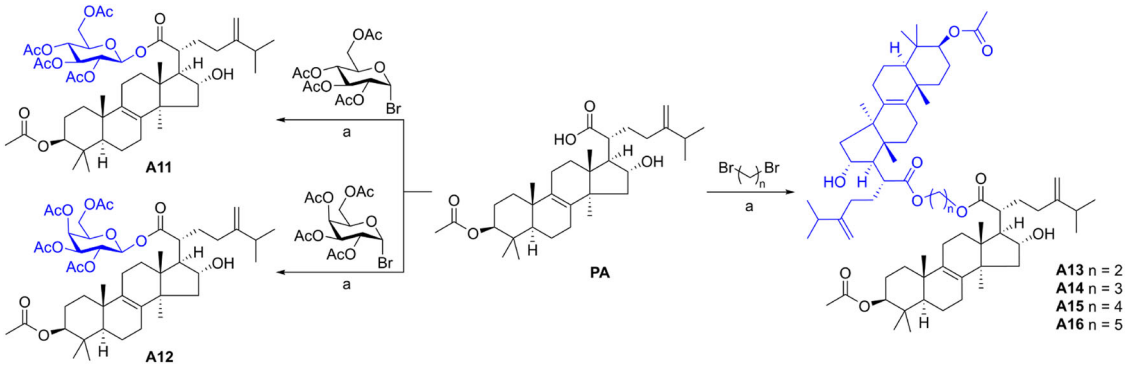

Scheme 2 Synthetic route of compounds **A11**-**A16**. Reagents and conditions: a K_2CO_3, DMF, room temperature

Scheme 3 Synthetic route of compounds **A17**-**A18**. Reagents and conditions: a LiOH, THF:MeOH:H_2O, 50 °C; b H_2, Pt/C, MeOH, room temperature

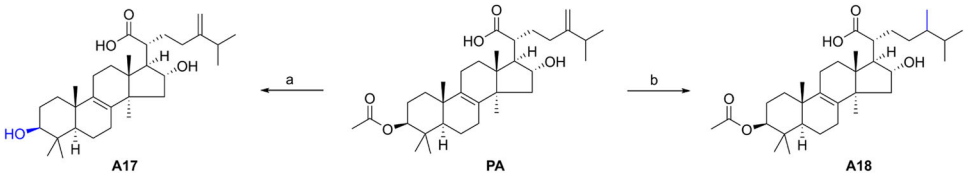

of PA, PA was esterified by two glycosyl bromides in the presence of potassium carbonate to give the corresponding carbohydrate derivatives **A11**-**A12**. The dimers of PA (**A13**-**A16**) were formed similarly to compound **A11** under the same conditions but using excess dibromoalkanes as starting materials. PA was hydrolyzed using LiOH in THF/MeOH/H_2O to obtain compound **A17**, which is also called tumulosic acid and is found in *Poria cocos* [8, 17]. PA was reduced by H_2/Pt-C in methanol to yield compound **A18**. The structures of the synthesized PA derivatives **A1**-**A18** were then characterized using ^{1}H NMR, ^{13}C NMR, and High-resolution mass spectrometry (HRMS).

Pharmacology

In vitro cytotoxicity

First, 18 PA derivatives were tested against two human tumor cell lines (HepG2 and HSC-2) to evaluate their in vitro cytotoxicity using the CCK-8 assay. PA and cisplatin were used as positive controls. The IC_{50} values of these compounds are listed in Table 1. The results of activity test showed that natural PA did not exhibit cytotoxicity against these two cell lines. Compared with the precursor PA, 8 out of 18 derivatives showed remarkable improvement in anticancer activity. These eight compounds showed better activity against HSC-2 cells than against HepG2 cells. Among them, derivatives **A5** and **A6** exhibited remarkable activity against HSC-2 cell line with IC_{50} values of 6.79 ± 0.23 μM and 9.69 ± 0.38 μM, respectively. Interestingly, compound **A11**, which contains a glucose group, showed good activity; however, **A12**, which contains a galactose group, showed no activity. Compound **A17** was the most potent molecule in cytotoxicity against HepG2 (IC_{50}: 7.36 ± 0.98 μM) and HSC-2 cell lines (IC_{50}: 2.50 ± 0.15 μM), showing better activities than positive control cisplatin.

Table 1 IC_{50} values of the tested compounds against HepG2 and HSC-2 cells[a]

compound	IC_{50} (μM)[b]	
	HepG2	HSC-2
A1	67.29 ± 2.48	28.20 ± 1.70
A5	19.17 ± 0.75	6.79 ± 0.23
A6	20.19 ± 0.53	9.69 ± 0.38
A7	22.15 ± 1.18	18.83 ± 8.89
A9	>100	73.55 ± 10.79
A11	30.31 ± 1.82	13.80 ± 6.36
A17	7.36 ± 0.98	2.50 ± 0.15
A18	28.16 ± 1.46	24.19 ± 12.09
PA	>100	>100
Cisplatin	9.44 ± 1.08	8.50 ± 0.94

[a]Data represent the mean of three experiments and are expressed as the mean ± SD

[b]IC_{50} value was defined as the concentration at which 50% cell survival was observed

Structure-activity relationship

The SAR of the PA derivatives was mined according to their in vitro cytotoxicity potential. Among the 21-COOH ester derivatives, benzyl compound **A1** displayed moderate cytotoxicity (HepG2 IC_{50}: 67.29 ± 2.48 μM; HSC-2 IC_{50}: 28.20 ± 1.70 μM), and compound **A11** containing a

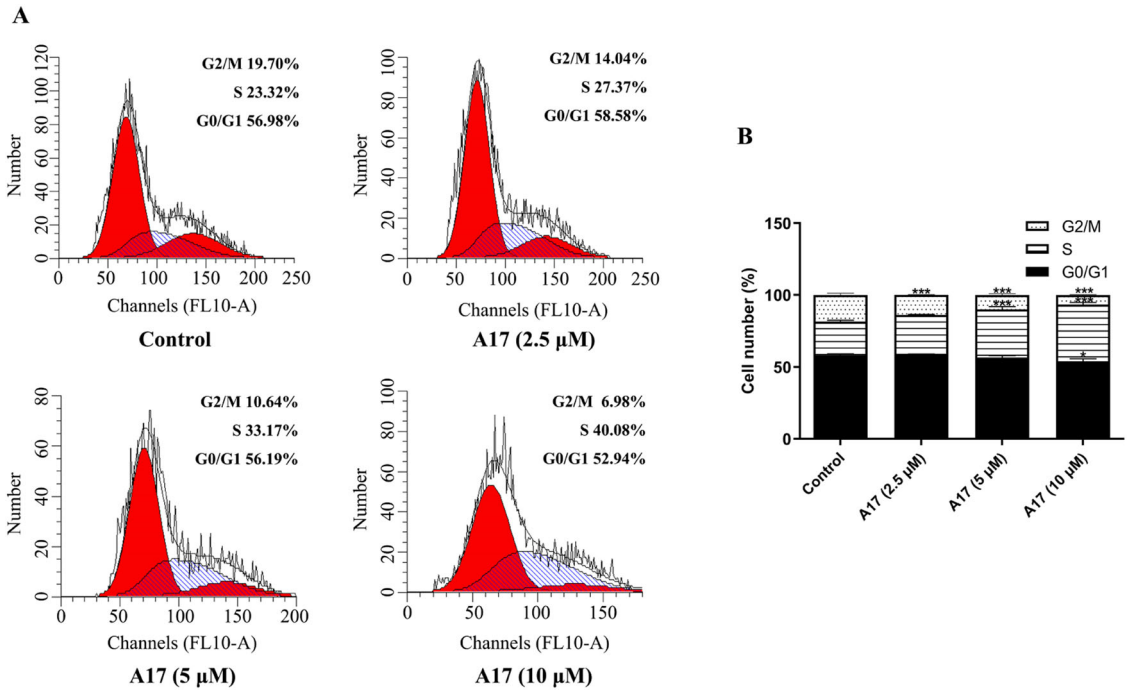

Fig. 2 Effects of **A17** on cell cycle distribution of HSC-2 cells. **A** Cell cycle distribution analysis of HSC-2 cells treated with 2.5, 5 and 10 μM **A17** for 48 h, following staining with PI by flow cytometry. **B** Quantification analysis. $*p < 0.05$, $***p < 0.001$ compared to control

glucose group resulted in good activity in tested cell lines, whereas alkyl compounds did not increase the activity of PA. In addition, alkyl compounds (**A5** and **A6**) containing a terminal OH group showed potent cytotoxicity against the two cancer cell lines. Moreover, no anticancer activity was observed for the PA dimers. Compound **A7** with a 3-OH group displayed moderate cytotoxicity against HepG2 and HSC-2 cell lines with IC_{50} values of 22.15 ± 1.18 μM and 18.83 ± 8.89 μM, respectively. For compounds **A8** and **A9**, the oxidation of hydroxyl to ketone considerably decreased their activity against the two cancer cell lines. To our surprise, compound **A17**, from the hydrolysis of a 3-acetoxy group in PA, showed the strongest cytotoxic activity against HepG2 and HSC-2 cells with IC_{50} values of 7.36 ± 0.98 μM and 2.50 ± 0.15 μM, respectively. In addition, compound **A18**, generated from the reduction of 31-alkene in PA, also demonstrated moderate anti-proliferative activity (HepG2 IC_{50}: 28.16 ± 1.46 μM; HSC-2 IC_{50}: 24.19 ± 12.09 μM).

Cell cycle analysis

To determine whether the cytotoxic potency of compound **A17** resulted from cell cycle arrest, the effects of **A17** on cell cycle distribution in HSC-2 cells were investigated by flow cytometry after labeling with propidium iodide (PI). The cells were treated with the vehicle and **A17** (2.5, 5, and 10 μM) for 48 h. As shown in Fig. 2, compared with the control group, treatment of HSC-2 cells with **A17** (2.5, 5, and 10 μM) induced cell cycle arrest at the S phase in a dose-dependent manner. These data suggest that cell cycle arrest by compound **A17** might be responsible for its anti-proliferative effect.

Apoptosis analysis

To further study the effects of the compound **A17** on oral HSC-2 cell apoptosis, flow cytometry was performed using an Annexin V-FITC/PI staining assay. The cells were treated with the vehicle and **A17** (2.5, 5, and 10 μM) for 48 h. As shown in Fig. 3, **A17** induced apoptosis of HSC-2 cells in a dose-dependent manner. After incubation with 2.5, 5, and 10 μM **A17**, the percentage of apoptotic cells was significantly higher than that in the control group. These data indicate that **A17** displays the anti-proliferative activity, probably through the induction of cell apoptosis.

Acridine orange/ethidium bromide (AO/EB) staining

Subsequently, AO/EB staining was used to confirm the apoptotic effect of compound **A17**. The HSC-2 cells were treated with vehicle and **A17** (2.5, 5, and 10 μM) for 48 h, then stained with AO/EB, after which images were taken using a fluorescent microscope (Fig. 4). The results revealed that, while cells in the control group maintained normal

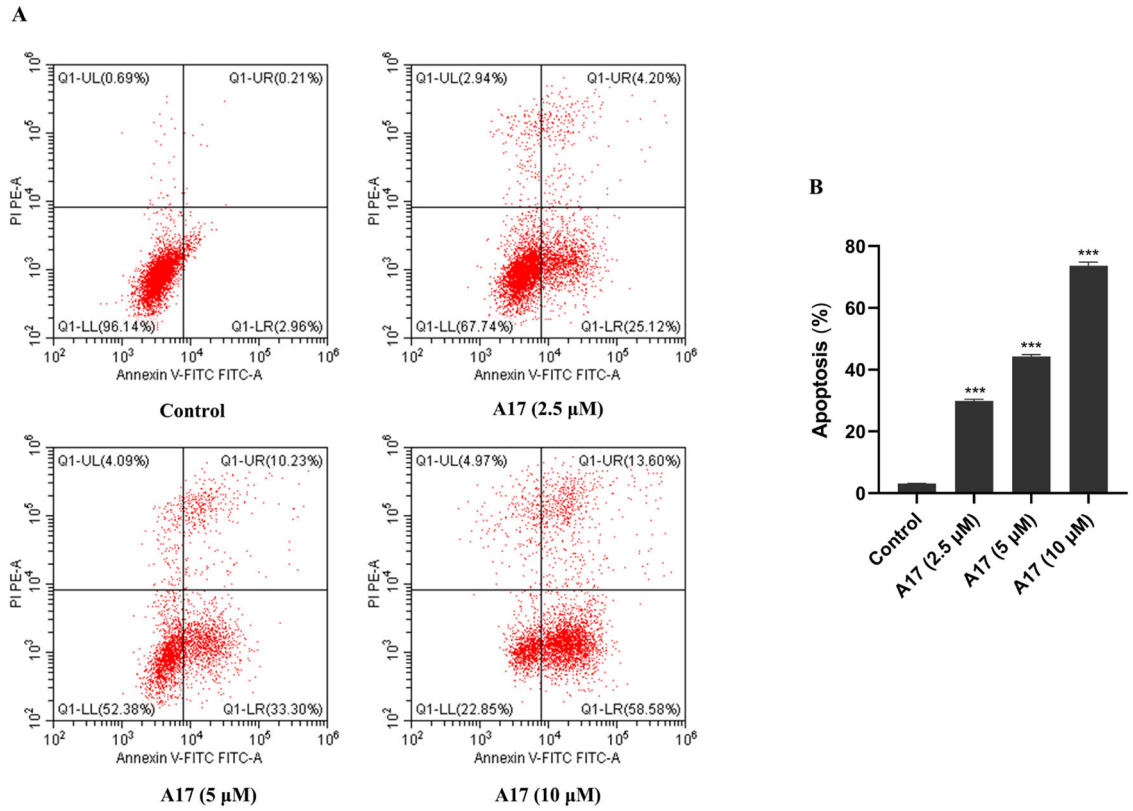

Fig. 3 **A17** induces apoptosis in HSC-2 cells. **A** Apoptosis analysis of HSC-2 cells treated with 2.5, 5, and 10 μM **A17** for 48 h, followed by staining with an Annexin V-FITC/PI by flow cytometry. **B** Quantification. ***$p < 0.001$ compared to control

morphology and displayed bright green fluorescence, apoptotic morphological hallmarks, including cell shrinkage and condensed chromatin, were observed in 5 and 10 μM **A17**-treated cells. These data highlight the apoptotic effects of **A17** on HSC-2 cells.

Western blot analysis of proteins involved in cell cycle and apoptosis

To further investigate the mechanisms underlying cycle arrest and apoptosis induced by **A17**, we determined the expression levels of CDK1, cyclinB1, Cleaved caspase 3, and Cleaved PARP1 in **A17**-treated HSC-2 cancer cells. The cells were treated with vehicle and **A17** (2.5, 5, and 10 μM) for 48 h, and then detected by western blotting. As shown in Fig. 5, our findings demonstrated that **A17** induced the up-regulation of CDK1 and cyclinB1 proteins expression in a dose-dependent manner. In addition, the cleaved forms of caspase 3 and PARP1 were increased in a dose-dependent manner in HSC-2 cells following treatment with compound **A17**. These results suggest that the cycle arrest and apoptosis induced by **A17** were at least partially mediated through the inhibition of CDKs and activation of the caspase cascade, respectively.

Western blot analysis of proteins involved in autophagy

Autophagy plays a crucial role in programmed cell death. Therefore, we investigated whether autophagy was involved in **A17**-reduced HSC-2 cell death. The cells were treated with vehicle and **A17** (2.5, 5, and 10 μM) for 48 h, and western blotting was used to determine the relative levels of the autophagy-related proteins Beclin1 and LC3. As shown in Fig. 6, after treatment with **A17**, the Beclin1 levels and ratio of LC3 II/I significantly increased in a dose-dependent manner, indicating autophagy. In addition, it was found that **A17** slightly affected total LC3 (I/II) protein expression at low concentrations. These results indicated that **A17** induces autophagy in oral HSC-2 cancer cells.

Western blot analysis of proteins involved in AKT and AMPK signaling

Many signaling pathways, such as AKT and AMPK, play vital roles in regulating cellular homeostasis and survival.

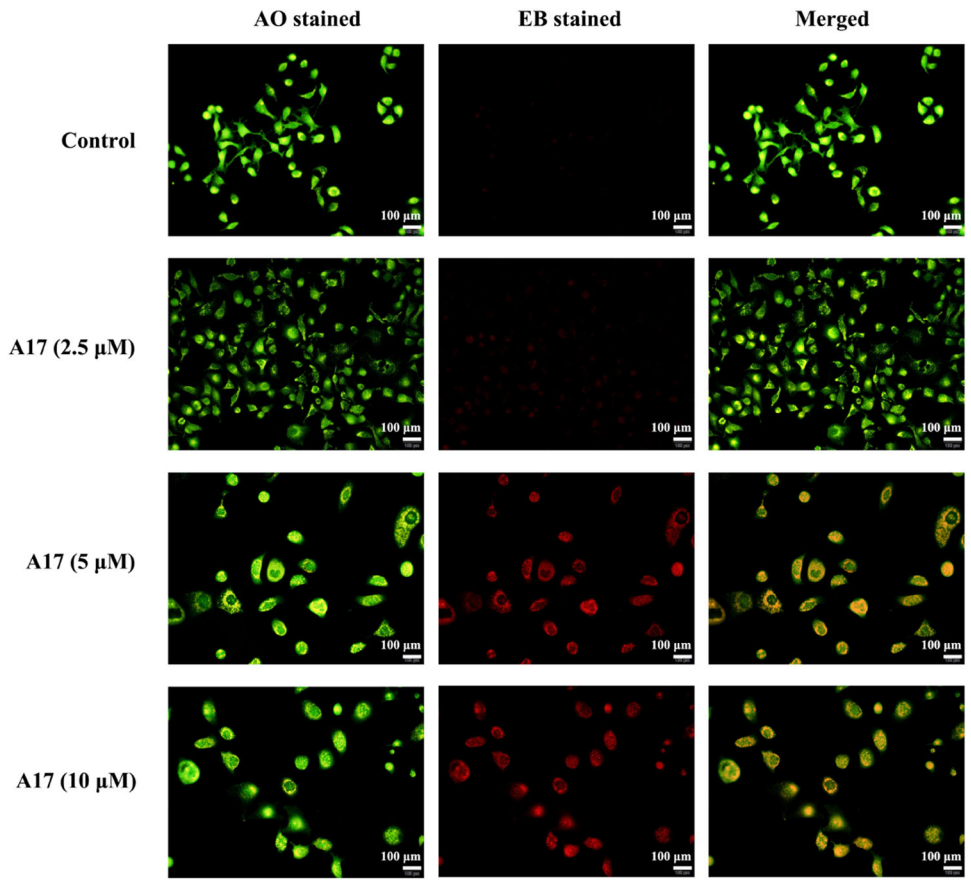

Fig. 4 AO/EB staining of HSC-2 cells treated with 2.5, 5 and 10 μM **A17** for 48 h. Scale bars 100 μm

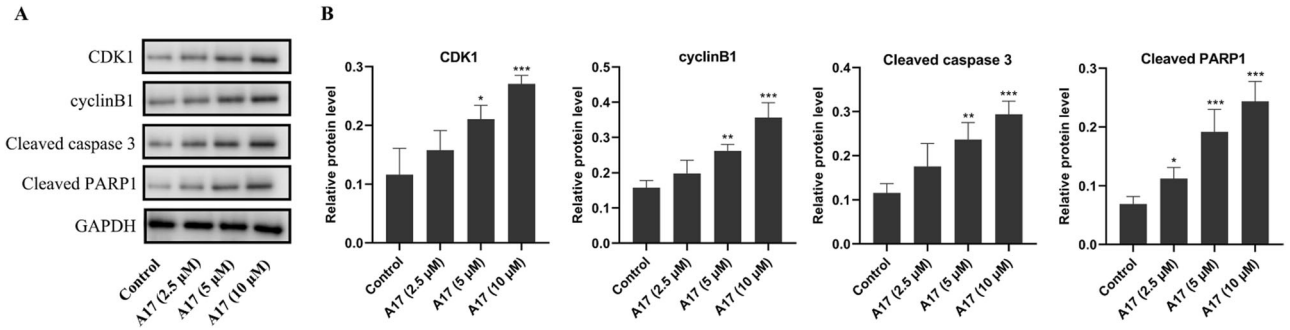

Fig. 5 Expression of CDK1, cyclinB1, Cleaved caspase 3, Cleaved PARP1 were evaluated by western blot in HSC-2 cells treated with compound **A17** for 48 h at different concentrations with GAPDH used as a reference. **A** Western blot analyses of the relative levels of CDK1, cyclinB1, Cleaved caspase 3, Cleaved PARP1. **B** Western blotting quantification. $^{*}p < 0.05$, $^{**}p < 0.01$, $^{***}p < 0.001$ compared to control

In this study, we further explored the effects of **A17** on AKT and AMPK signaling in HSC-2 cells. The cells were treated with vehicle and **A17** (2.5, 5, and 10 μM) for 48 h, and western blotting was performed to determine the relative levels of p-AKT and p-AMPK. As shown in Fig. 7, the expression levels of p-AKT and p-AMPK were significantly upregulated by **A17** in a dose-dependent manner. These results indicate that **A17** exhibits cytotoxicity, probably by activating AKT and AMPK signaling in HSC-2 cells.

Conclusions

In conclusion, eighteen derivatives of PA were successfully synthesized, characterized, and evaluated for cytotoxicity against two human cancer cell lines using the CCK-8 assay. Preliminary in vitro anticancer study presented compound **A17**, namely tumulosic acid, as the most potent derivative against HepG2 and HSC-2 cells, with IC_{50} values of 7.36 ± 0.98 and 2.50 ± 0.15 μM, respectively, whereas the parent PA showed no anticancer

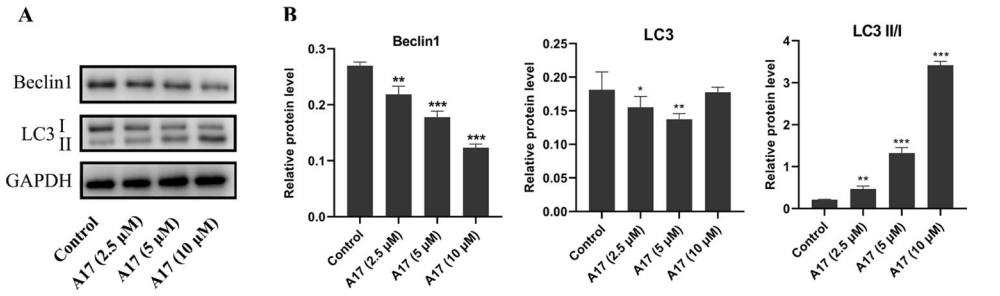

Fig. 6 Compound **A17** induced HSC-2 cells autophagy. **A** Expressions of Beclin1 and LC3 (I/II) were evaluated by western blot in HSC-2 cells treated with compound **A17** for 48 h at different concentrations with GAPDH used as a reference. **B** Western blotting quantification. $*p < 0.05$, $**p < 0.01$, $***p < 0.001$ compared to control

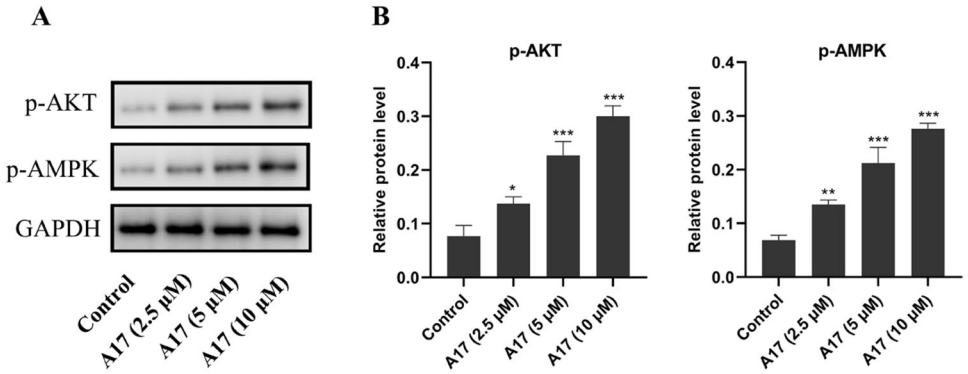

Fig. 7 Compound **A17** activated AKT and AMPK signaling. **A** Expression of p-AKT and p-AMPK were evaluated by western blotting in HSC-2 cells treated with compound **A17** for 48 h at different concentrations with GAPDH as a reference. **B** Western blotting quantification. $*p < 0.05$, $**p < 0.01$, $***p < 0.001$ compared to control

activity against above cell lines. Additionally, **A17** displayed superior cytotoxic potency compared to cisplatin. Corroboration of the SAR was achieved based on cytotoxicity results. Flow cytometry analysis revealed that **A17** efficiently induced HSC-2 cell cycle arrest at the S phase and cell apoptosis. AO/EB staining further confirmed the apoptotic effect of **A17**. Western blotting analysis demonstrated that the apoptotic mechanism of compound **A17** was mediated by changes in Cleaved caspase 3 and Cleaved PARP1 levels, while the cell cycle arrest mechanism involved changes in CDK1 and cyclinB1. Beclin1 and the LC3 II/I ratio were involved in the regulation of HSC-2 cell autophagy by compound **A17**. Our findings revealed that **A17** also affected the AKT and AMPK pathways. Several previous studies have reported that **A17** showed moderate anti-proliferative activity against three leukemic cell lines (MOLT-4, CCRF-CEM, and HL-60) [8], exhibited moderate cytotoxicity against HT-29 cancer cells via inhibition of topoisomerase I/II [17], and induced apoptosis via the mitochondria-mediated pathway in lung A549 cancer cells [30]. To the best of our knowledge, our study is the first to report the structural modification of PA, SARs, and underlying anticancer molecular mechanisms against human oral HSC-2 cells, including cell cycle arrest, apoptosis, autophagy, and signaling pathways. In addition, **A17** showed significant anticancer activity against HSC-2 cells, suggesting that it may be a potential chemotherapeutic candidate for oral cancer treatment.

Experimental

Materials

PA was obtained from Chengdu Pufei De Biotech Co. Ltd. (Chengdu, China). All other chemical reagents were analytically pure, purchased from commercial suppliers, and used without treatment unless otherwise noted. ^{1}H and ^{13}C NMR spectra were tested using a 400-MHz Agilent DD2400-MR instrument, and the chemical shifts (δ) were recorded in ppm and coupling constants (J) in Hz, using TMS as an internal standard. High-resolution mass spectrometry (HRMS) was performed using a Waters Xevo G2-S QTOF instrument. Melting points (uncorrected) were measured using an SGWX-4 microscope melting-point apparatus. Thin-layer chromatography (TLC) was performed on silica gel plates (Silica Gel 60 GF254) and visualized under UV light (254 and 365 nm). Flash chromatography was performed using silica gel (200–300 mesh).

Chemistry

General procedure for the synthesis of compounds A1-A6

To the solution of PA (0.09 mmol) in *N*,*N*-dimethylformamide (2 mL) were added corresponding halogenated

hydrocarbon (0.18 mmol) and potassium carbonate (0.18 mmol). The mixture was then stirred at room temperature for 2 h. The reaction was quenched with an ammonium chloride solution and extracted with dichloromethane. The combined organic layers were washed with water and brine, dried over anhydrous sodium sulfate and concentrated in a vacuum. The crude product was purified by column chromatography to obtain the desired products **A1**-**A6**.

3β-Acetoxy-16α-hydroxy-lanosta-8,24(31)-diene-21-oic acid-benzyl ester (A1)

White solid; m.p.: 169–170 °C; yield 78%; ^{1}H (400 MHz, $CDCl_3$): δ 7.38-7.29 (m, 5H), 5.16 (d, $J = 12.2$ Hz, 1H), 5.05 (d, $J = 12.2$ Hz, 1H), 4.71 (s, 1H), 4.63 (s, 1H), 4.48 (dd, $J = 4.1$, 11.5 Hz, 1H), 4.11-4.06 (m, 1H), 2.48 (dt, $J = 2.7$, 11.0 Hz, 1H), 2.18-2.10 (m, 3H), 2.03 (s, 3H), 1.99-1.77 (m, 9H), 1.69-1.46 (m, 6H), 1.31-1.24 (m, 2H), 1.14-1.06 (m, 5H), 0.95-0.91 (m, 9H), 0.86 (s, 6H), 0.69 (s, 3H); ^{13}C (100 MHz, $CDCl_3$): δ 175.60, 171.07, 155.04, 135.75, 134.24, 134.06, 128.59, 128.49, 128.21, 106.75, 80.78, 77.05, 65.98, 56.85, 50.37, 48.04, 47.07, 45.88, 42.71, 37.76, 36.83, 35.10, 33.64, 32.11, 30.66, 28.85, 27.87, 26.36, 25.14, 24.07, 21.81, 21.70, 21.34, 20.39, 19.10, 17.97, 17.39, 16.52; HRMS (ESI): calculated for $C_{40}H_{58}O_5Na$ $[M + Na]^+$ 641.4176, found 641.4173.

3β-Acetoxy-16α-hydroxy-lanosta-8,24(31)-diene-21-oic acid-ethyl ester (A2)

White solid; mp: 147–148 °C; yield 82%; ^{1}H (400 MHz, $CDCl_3$): δ 4.73 (s, 1H), 4.68 (s, 1H), 4.47 (dd, $J = 4.2$, 11.5 Hz, 1H), 4.15–4.06 (m, 3H), 2.45–2.38 (m, 1H), 2.24–2.07 (m, 3H), 2.03–1.87 (m, 10H), 1.83–1.46 (m, 8H), 1.30–1.24 (m, 5H), 1.22–1.14 (m, 2H), 1.09 (s, 3H), 1.00–0.95 (m, 9H), 0.86 (s, 3H), 0.85 (s, 3H), 0.70 (s, 3H); ^{13}C (100 MHz, $CDCl_3$): δ 175.81, 171.04, 155.11, 134.23, 134.10, 106.82, 80.77, 77.07, 59.99, 56.86, 50.36, 48.04, 47.01, 45.91, 42.65, 37.74, 36.84, 35.10, 33.63, 32.12, 30.66, 28.86, 27.86, 26.35, 25.15, 24.05, 21.81, 21.68, 21.32, 20.40, 19.09, 17.96, 17.39, 16.50, 14.23; HRMS (ESI): calculated for $C_{35}H_{56}O_5Na$ $[M + Na]^+$ 579.4019, found 579.4022.

3β-Acetoxy-16α-hydroxy-lanosta-8,24(31)-diene-21-oic acid-propyl ester (A3)

White solid; mp: 135–136 °C; yield 83%; ^{1}H (400 MHz, $CDCl_3$): δ 4.73 (s, 1H), 4.68 (s, 1H), 4.47 (dd, $J = 4.2$, 11.5 Hz, 1H), 4.11–4.3.94 (m, 3H), 2.46–2.10 (m, 1H), 2.24–2.07 (m, 3H), 2.03–1.87 (m, 10H), 1.84–1.77 (m, 1H), 1.73–1.46 (m, 9H), 1.31–1.14 (m, 4H), 1.10 (s, 3H), 1.00–0.93 (m, 12H), 0.86 (s, 3H), 0.86 (s, 3H), 0.70 (s, 3H); ^{13}C (100 MHz, $CDCl_3$): δ 175.93, 171.05, 155.12, 134.24, 134.10, 106.79, 80.77, 77.10, 65.77, 56.90, 50.37, 48.04, 47.10, 45.90, 42.66, 37.75, 36.84, 35.10, 33.67, 32.16, 30.67, 28.82, 27.86, 26.35, 25.14, 24.05, 21.86, 21.82, 21.69, 21.33, 20.40, 19.09, 17.96, 17.35, 16.50, 10.63; HRMS (ESI): calculated for $C_{36}H_{58}O_5Na$ $[M + Na]^+$ 593.4176, found 593.4180.

3β-Acetoxy-16α-hydroxy-lanosta-8,24(31)-diene-21-oic acid-isopropyl ester (A4)

White solid; mp: 153–154 °C; yield 75%; ^{1}H (400 MHz, $CDCl_3$): δ 5.02 (septet, $J = 6.2$ Hz, 1H), 4.74 (s, 1H), 4.68 (s, 1H), 4.48 (dd, $J = 4.2$, 11.5 Hz, 1H), 4.09 (t, $J = 7.0$ Hz, 1H), 2.42–2.36 (m, 1H), 2.25–2.07 (m, 3H), 2.04–1.84 (m, 10H), 1.83–1.66 (m, 6H), 1.61–1.47 (m, 2H), 1.32–1.28 (m, 1H), 1.26–1.23 (m, 8H), 1.15–1.12 (m, 1H), 1.10 (s, 3H), 1.01–0.96 (m, 9H), 0.87 (s, 3H), 0.86 (s, 3H), 0.71 (s, 3H); ^{13}C (100 MHz, $CDCl_3$): δ 175.29, 171.04, 155.22, 134.23, 134.16, 106.79, 80.77, 77.09, 67.36, 56.76, 50.37, 48.05, 47.15, 46.00, 42.60, 37.75, 36.85, 35.12, 33.71, 32.01, 30.85, 29.01, 27.87, 26.35, 25.20, 24.06, 21.93, 21.84, 21.70, 21.33, 20.40, 19.11, 17.97, 17.41, 16.52; HRMS (ESI): calculated for $C_{36}H_{58}O_5Na$ $[M + Na]^+$ 593.4176, found 593.4177.

3β-Acetoxy-16α-hydroxy-lanosta-8,24(31)-diene-21-oic acid-hydroxyethyl ester (A5)

White solid; mp: 147–148 °C; yield 83%; ^{1}H (400 MHz, $CDCl_3$): δ 4.74 (s, 1H), 4.68 (s, 1H), 4.48–4.45 (m, 1H), 4.23–4.14 (m, 2H), 4.12–4.07 (m, 1H), 3.82 (t, $J = 4.0$ Hz, 2H), 2.50–2.45 (m, 1H), 2.27–2.09 (m, 4H), 2.03–1.90 (m, 11H), 1.84–1.46 (m, 7H), 1.29–1.22 (m, 2H), 1.19–1.14 (m, 2H), 1.09 (s, 3H), 1.01–0.95 (m, 9H), 0.85 (s, 6H), 0.70 (s, 3H); ^{13}C (100 MHz, $CDCl_3$): δ 176.23, 171.14, 154.98, 134.25, 134.03, 106.93, 80.77, 76.92, 65.83, 61.07, 56.80, 50.34, 48.04, 46.88, 45.89, 42.67, 37.74, 36.84, 35.07, 33.62, 32.17, 30.52, 28.92, 27.86, 26.34, 25.16, 24.04, 21.82, 21.69, 21.35, 20.40, 19.10, 17.95, 17.49, 16.51; HRMS (ESI): calculated for $C_{35}H_{56}O_6Na$ $[M + Na]^+$ 595.3969, found 595.3971.

3β-Acetoxy-16α-hydroxy-lanosta-8,24(31)-diene-21-oic acid-hydroxypropyl ester (A6)

Colorless viscous solid; mp: 61–62 °C; yield 87%; ^{1}H (400 MHz, $CDCl_3$): δ 4.74 (s, 1H), 4.67 (s, 1H), 4.47 (dd, $J = 4.2$, 11.3 Hz, 1H), 4.26–4.13 (m, 2H), 4.11–4.07 (m, 1H), 3.72 (t, $J = 5.9$ Hz, 2H), 2.47–2.41 (m, 1H), 2.23–2.07 (m, 4H), 2.03 (s, 3H), 1.99–1.97 (m, 2H), 1.94–1.86 (m, 6H), 1.82–1.74 (m, 2H), 1.72–1.64 (m, 4H), 1.60–1.46 (m,

2H), 1.29–1.22 (m, 3H), 1.19–1.14 (m, 2H), 1.09 (s, 3H), 1.00–0.95 (m, 9H), 0.85 (s, 6H), 0.69 (3H); ^{13}C (100 MHz, $CDCl_3$): δ 176.19, 171.13, 154.99, 134.23, 134.06, 106.91, 80.79, 61.21, 59.34, 56.85, 50.34, 48.04, 47.02, 45.86, 42.67, 37.74, 36.84, 35.08, 33.65, 32.20, 31.55, 30.57, 28.88, 27.87, 26.34, 25.15, 24.05, 21.83, 21.70, 21.35, 20.41, 19.11, 17.95, 17.40, 16.51; HRMS (ESI): calculated for $C_{36}H_{58}O_6Na$ $[M + Na]^+$ 609.4125, found 609.4125.

Procedure for the synthesis of compound A7

Compound **A1** (0.08 mmol) and sodium borohydride (0.8 mmol) were dissolved in anhydrous alcohol (3 mL). The reaction mixture was refluxed for 4 h under an argon atmosphere, followed by concentration in a vacuum. The resulting residue was purified using flash column chromatography to obtain compound **A7**.

3β,16α-Dihydroxy-lanosta-8,24(31)-diene-21-oic acid-benzyl ester (A7)

White solid; mp: 172–174 °C; yield 58%; ^{1}H (400 MHz, $CDCl_3$): δ 7.39–7.31 (m, 5H), 5.16 (d, $J = 12.2$ Hz, 1H), 5.07 (d, $J = 12.2$ Hz, 1H), 4.72 (s, 1H), 4.63 (s, 1H), 4.16–4.07 (m, 2H), 3.22 (dd, $J = 4.0$ 11.4 Hz, 1H), 2.51–2.45 (m, 1H), 2.20–2.10 (m, 3H), 2.04–1.79 (m, 9H), 1.69–1.64 (m, 3H), 1.61–1.54 (m, 2H), 1.52–1.41 (m, 2H), 1.30–1.22 (m, 3H), 1.09 (s, 3H), 0.99 (m, 3H), 0.96–0.92 (m, 9H), 0.79 (s, 3H), 0.69 (s, 3H); ^{13}C (100 MHz, $CDCl_3$): δ 175.65, 155.06, 135.72, 134.41, 133.95, 128.61, 128.52, 128.25, 106.77, 78.84, 77.16, 66.03, 56.96, 50.24, 48.04, 46.97, 45.92, 42.69, 38.85, 36.95, 35.42, 33.64, 32.10, 30.74, 28.87, 27.94, 27.71, 26.45, 25.14, 21.81, 21.69, 20.39, 19.07, 18.09, 17.41, 15.43; HRMS (ESI): calculated for $C_{38}H_{56}O_4Na$ $[M + Na]^+$ 599.4070, found 599.4069.

General procedure for the synthesis of compound A8

Compound **A7** (0.11 mmol) was dissolved in dichloromethane (3 mL). Dess-Martin periodinane (0.33 mmol) was then added. The reaction mixture was stirred at room temperature for 3 h under an argon atmosphere. The mixture was quenched with saturated sodium sulfite and extracted with dichloromethane. The combined organic layers were washed with brine, dried over sodium sulfate, filtered, and concentrated in a vacuum. The residue was purified by flash column chromatography to yield compound **A8**.

3,16-Dione-lanosta-8,24(31)-diene-21-oic acid-benzyl ester *(A8)*

White solid; mp: 102–104 °C; yield 60%; ^{1}H (400 MHz, $CDCl_3$): δ 7.39–7.31 (m, 5H), 5.20 (d, $J = 12.2$ Hz, 1H), 5.05 (d, $J = 12.2$ Hz, 1H), 4.72 (s, 1H), 4.66 (s, 1H), 2.69–2.53 (m, 4H), 2.44–2.38 (m, 1H), 2.33 (d, $J = 18.3$ Hz, 1H), 2.21–2.04 (m, 2H), 1.98–1.88 (m, 6H), 1.86–1.81 (m, 1H), 1.71–1.64 (m, 2H), 1.66–1.59 (m, 2H), 1.44–1.32 (m, 1H), 1.28–1.23 (m, 2H), 1.11–1.05 (m, 12H), 0.97–0.93 (m, 6H), 0.79 (s, 3H); ^{13}C (100 MHz, $CDCl_3$): δ 217.59, 217.31, 174.40, 154.82, 135.45, 134.63, 132.29, 128.76, 128.55, 128.37, 106.88, 66.23, 57.27, 50.94, 47.36, 46.38, 44.06, 43.90, 43.42, 37.00, 35.71, 34.46, 33.54, 31.92, 29.78, 28.46, 26.70, 26.09, 24.97, 21.81, 21.72, 21.30, 20.11, 19.21, 18.59, 16.98; HRMS (ESI): calculated for $C_{38}H_{52}O_4Na$ $[M + Na]^+$ 595.3757, found 595.3759.

General procedure for the synthesis of compound *A9*

Compound **A1** (0.08 mmol) was dissolved in dichloromethane (3 mL) to which Dess-Martin periodinane (0.15 mmol) was added. The reaction mixture was stirred at room temperature for 3 h under an argon atmosphere. The mixture was quenched with saturated sodium sulfite and extracted with dichloromethane. The combined organic layers were washed with brine (10 mL), dried over sodium sulfate, filtered, and concentrated in a vacuum. The residue was purified by flash column chromatography to yield compound **A9**.

3β-Acetoxy-16-one-lanosta-8,24(31)-diene-21-oic acid-benzyl ester *(A9)*

White solid; mp: 142–144 °C; yield 100%; ^{1}H (400 MHz, $CDCl_3$): δ 7.38–7.31 (m, 5H), 5.20 (d, $J = 12.1$ Hz, 1H), 5.04 (d, $J = 12.1$ Hz, 1H), 4.71 (s, 1H), 4.65 (s, 1H), 4.49 (dd, $J = 4.1$, 11.6 Hz, 1H), 2.69–2.62 (m, 1H), 2.58–2.51 (m, 2H), 2.30 (d, $J = 18.2$ Hz, 1H), 2.20–2.14 (m, 1H), 2.05 (s, 3H), 1.96–1.87 (m, 4H), 1.84–1.75 (m, 2H), 1.72–1.51 (m, 6H), 1.36–1.21 (m, 4H), 1.16–1.12 (m, 2H), 1.04 (s, 3H), 0.98–0.93 (m, 9H), 0.88 (s, 6H), 0.77 (s, 3H); ^{13}C (100 MHz, $CDCl_3$): δ 217.91, 174.41, 171.03, 154.84, 135.72, 135.46, 131.43, 128.75, 128.55, 128.36, 106.85, 80.60, 66.21, 57.28, 50.26, 46.34, 44.09, 43.91, 43.26, 37.75, 37.00, 34.93, 33.52, 31.93, 29.74, 28.46, 27.87, 26.75, 24.93, 24.00, 21.81, 21.72, 21.36, 20.04, 19.11, 17.91, 16.88, 16.52; HRMS (ESI): calculated for $C_{40}H_{56}O_5Na$ $[M + Na]^+$ 639.4019, found 639.4015.

Procedure for the synthesis of compound A10

Compound **A9** (0.16 mmol) was dissolved in methanol (30 mL). Subsequently, 10% Pt/C (100 mg) was added. The mixture was stirred overnight at room temperature under a hydrogen atmosphere. The reaction mixture was filtered and concentrated to yield compound **A10**.

3β-Acetoxy-16-one-lanosta-8-ene-21-oic acid-benzyl ester (A10)

White solid; mp: 201–203 °C; yield 98%; ^{1}H (400 MHz, Pyridin-d_5): δ 4.66 (dd, $J = 4.4$, 11.6 Hz, 1H), 2.97–2.83 (m, 3H), 2.53 (d, $J = 18.0$ Hz, 1H), 2.24–2.16 (m, 1H), 2.06–2.02 (m, 5H), 1.95–1.89 (m, 4H), 1.73–1.43 (m, 9H), 1.33–1.24 (m, 1H), 1.13–1.05 (m, 8H), 0.93–0.91 (9H), 0.88–0.75 (m, 9H); ^{13}C (100 MHz, Pyridin-d_5): δ 170.36, 135.52, 131.89, 80.20, 57.75, 50.24, 46.44, 44.22, 43.41, 38.72, 38.51, 37.71, 36.95, 34.82, 32.26, 32.13, 31.32, 28.72, 27.69, 26.68, 24.73, 24.09, 20.90, 20.53, 20.14, 18.87, 18.10, 17.97, 17.17, 16.86, 16.50, 15.26, 15.11; HRMS (ESI): calculated for $C_{33}H_{52}O_5Na$ $[M + Na]^+$ 551.3706, found 551.3706.

General procedure for the synthesis of compounds A11/A12

PA (0.09 mmol) was dissolved in *N*,*N*-dimethylformamide (2 mL). Glycosyl bromide (0.18 mmol) and potassium carbonate (0.18 mmol) were then added. The reaction mixture was stirred at room temperature for 2 h under an argon atmosphere. The reaction was quenched with an ammonium chloride solution and extracted with dichloromethane. The combined organic layers were washed with water and brine, dried over anhydrous sodium sulfate, and concentrated in a vacuum. The crude product was purified by column chromatography to yield the desired products **A11/A12**.

Pachymic acid 21-O-2,3,4,6-tetra-O-acetyl-β-D-glucopyranosyl ester (A11)

White solid; mp: 237–239 °C; yield 69%; ^{1}H (400 MHz, $CDCl_3$): δ 5.68 (d, $J = 7.9$ Hz, 1H), 5.28–5.10 (m, 3H), 4.73 (s, 3H), 4.65 (s, 3H), 4.46 (dd, $J = 4.0$, 11.4 Hz, 1H), 4.20 (dd, $J = 4.2$, 12.4 Hz, 1H), 4.09-4.03 (m, 2H), 3.83–3.79 (m, 1H), 2.46 (t, $J = 11.0$ Hz, 1H), 2.21–2.06 (m, 4H), 2.02–1.96 (m, 18H), 1.93–1.62 (m, 9H), 1.58–1.40 (m, 2H), 1.31–1.23 (m, 2H), 1.18–1.08 (m, 5H), 0.97–0.94 (m, 6H), 0.90 (s, 3H), 0.85 (s, 3H), 0.84 (s, 3H), 0.61 (s, 3H); ^{13}C (100 MHz, $CDCl_3$): δ 174.31, 171.01, 170.54, 170.17, 169.38, 168.98, 154.74, 134.21, 134.05, 106.69, 91.51, 80.65, 76.90, 72.91, 72.35, 69.91, 67.74, 61.44, 56.47, 50.34, 48.02, 46.29, 45.86, 42.62, 37.72, 36.80, 35.06, 34.08, 31.05, 30.63, 29.25, 27.85, 26.35, 25.04, 24.01, 21.69, 21.60, 21.31, 20.59, 20.57, 20.43, 19.10, 17.93, 17.69, 16.50; HRMS (ESI): calculated for $C_{47}H_{70}O_{14}Na$ $[M + Na]^+$ 881.4657, found 881.4639.

Pachymic acid 21-O-2,3,4,6-tetra-O-acetyl-β-D-galactopyranosyl ester (A12)

White solid; mp: 95–97 °C; yield 93%; ^{1}H (400 MHz, $CDCl_3$): δ 5.67 (d, $J = 8.4$ Hz, 1H), 5.39 (d, $J = 3.3$ Hz, 1H), 5.35 (dd, 8.5, 10.4 Hz, 1H), 5.05 (dd, $J = 3.4$, 10.4 Hz, 1H), 4.73 (s, 1H), 4.66 (s, 1H), 4.45 (dd, $J = 4.2$, 11.4 Hz, 1H), 4.13–4.00 (m, 5H), 2.50–2.44 (m, 1H), 2.20–2.08 (m, 6H), 2.01 (s, 6H), 1.99–1.96 (m, 12H), 1.86–1.72 (m, 3H), 1.67–1.63 (m, 3H), 1.57–1.43 (m, 2H), 1.27–1.20 (m, 3H), 1.09 (s, 3H), 0.99–0.95 (m, 6H), 0.90 (3H), 0.84 (s, 3H), 0.83 (s, 3H), 0.61 (s, 3H); ^{13}C (100 MHz, $CDCl_3$): δ 174.40, 170.99, 170.30, 170.19, 169.96, 169.08, 154.80, 134.25, 134.02, 106.77, 91.93, 80.64, 76.82, 71.34, 70.97, 67.45, 66.75, 60.81, 56.37, 50.34, 48.02, 46.17, 45.87, 42.57, 37.72, 36.80, 35.09, 33.94, 31.24, 30.68, 29.20, 27.84, 26.34, 25.05, 23.99, 21.73, 21.62, 21.29, 20.72, 20.64, 20.59, 20.53, 19.10, 17.93, 17.70, 16.49, 14.16; HRMS (ESI): calculated for $C_{47}H_{70}O_{14}Na$ $[M + Na]^+$ 881.4657, found 881.4651.

General procedure for the synthesis of compounds A13-A16

Dibromoalkane (0.07 mmol) and potassium carbonate (0.14 mmol) were added to the solution of PA (0.15 mmol) in *N*,*N*-dimethylformamide (5 mL). The reaction mixture was then stirred at room temperature for 3 h. The reaction was quenched with an ammonium chloride solution and extracted with dichloromethane. The combined organic layers were washed with water and brine, dried over anhydrous sodium sulfate, and concentrated in a vacuum. The crude product was purified by column chromatography to obtain the desired products **A13-A16**.

Ethyl-3β-acetoxy-16α-hydroxy-lanosta-8,24(31)-diene-21-oate (A13)

White solid; mp: 249–250 °C; yield 36%; ^{1}H (400 MHz, $CDCl_3$): δ 4.74 (s, 1H), 4.68 (s, 1H), 4.67 (dd, $J = 4.1$, 11.4 Hz, 1H), 4.31–4.23 (m, 2H), 4.11–4.06 (m, 1H), 4.49–4.43 (m, 1H), 2.23–2.08 (m, 3H), 2.03 (s, 3H), 2.00–1.90 (m, 6H), 1.83–1.40 (m, 8H), 1.31–1.22 (m, 3H), 1.17–1.11 (m, 2H), 1.09 (s, 3H), 1.00–0.95 (m, 9H), 0.86 (s, 3H), 0.85 (s, 3H), 0.69 (s, 3H); ^{13}C (100 MHz, $CDCl_3$): δ 175.73, 171.06, 154.83, 134.19, 134.07, 107.07, 80.72, 76.97, 61.85, 56.87, 50.35, 48.03, 46.75, 45.85, 42.71, 37.75, 36.84, 35.08, 33.53, 32.28, 30.60, 29.02, 27.85, 26.35, 25.17, 24.06, 21.87, 21.74, 21.34, 20.42, 19.10, 17.95, 17.45, 16.51; HRMS (ESI): calculated for $C_{68}H_{106}O_{10}Na$ $[M + Na]^+$ 1105.7678, found 1105.7634.

Propyl-3β-acetoxy-16α-hydroxy-lanosta-8,24(31)-diene-21-oate (A14)

White solid; mp: 104–105 °C; yield 40%; ^{1}H (400 MHz, $CDCl_3$): δ 4.73 (s, 1H), 4.67 (s, 1H), 4.67 (dd, $J = 4.0$, 11.4 Hz, 1H), 4.21–4.06 (m, 3H), 2.44 (t, $J = 11.0$ Hz, 1H), 2.23–2.15 (m, 3H), 2.03 (s, 3H), 2.01–1.86 (m, 7H),

1.82–1.40 (m, 8H), 1.31–1.22 (m, 3H), 1.16–1.10 (m, 2H), 1.09 (s, 3H), 1.00–0.95 (m, 9H), 0.86 (s, 3H), 0.85 (s, 3H), 0.69 (s, 3H); ^{13}C (100 MHz, $CDCl_3$): δ 175.65, 171.06, 154.87, 134.21, 134.07, 106.99, 80.75, 60.79, 56.82, 50.35, 48.05, 46.99, 45.86, 42.71, 37.74, 36.83, 35.09, 33.59, 32.24, 30.61, 28.93, 28.07, 27.86, 26.34, 25.15, 24.05, 21.85, 21.72, 21.34, 20.40, 19.11, 17.95, 17.40, 16.51; HRMS (ESI): calculated for $C_{69}H_{108}O_{10}Na$ $[M + Na]^+$ 1119.7834, found 1119.7801.

N-butyl-3β-acetoxy-16α-hydroxy-lanosta-8,24(31)-diene-21-oate (A15)

White solid; mp: 100–101 °C; yield 44%; ^{1}H (400 MHz, $CDCl_3$): δ 4.73 (s, 1H), 4.67 (s, 1H), 4.67 (dd, $J = 4.2$, 11.4 Hz, 1H), 4.21–4.07 (m, 3H), 2.43 (t, $J = 11.0$ Hz, 1H), 2.23–2.07 (m, 3H), 2.03 (s, 3H), 1.97–1.89 (m, 6H), 1.86–1.63 (m, 8H), 1.60–1.35 (m, 2H), 1.31–1.22 (m, 3H), 1.16–1.10 (m, 2H), 1.09 (s, 3H), 1.00–0.95 (m, 9H), 0.85 (s, 6H), 0.69 (s, 3H); ^{13}C (100 MHz, $CDCl_3$): δ 175.81, 171.07, 154.94, 134.20, 134.10, 106.92, 80.76, 63.58, 56.79, 50.36, 48.04, 47.10, 45.83, 42.71, 37.74, 36.83, 35.11, 33.61, 32.24, 30.61, 28.91, 27.85, 26.36, 25.35, 25.17, 24.05, 21.84, 21.72, 21.34, 20.40, 19.11, 17.95, 17.37, 16.50; HRMS (ESI): calculated for $C_{70}H_{110}O_{10}Na$ $[M + Na]^+$ 1133.7991, found 1133.7967.

N-pentyl-3β-acetoxy-16α-hydroxy-lanosta-8,24(31)-diene-21-oate (A16)

White solid; mp: 100–102 °C; yield 38%; ^{1}H (400 MHz, $CDCl_3$): δ 4.71 (s, 1H), 4.65 (s, 1H), 4.45 (dd, $J = 4.2$, 11.4 Hz, 1H), 4.10–4.04 (m, 2H), 4.01–3.95 (m, 1H), 2.40 (t, $J = 11.1$ Hz, 1H), 2.21–2.05 (m, 3H), 2.01 (s, 3H), 1.96–1.87 (m, 6H), 1.85–1.76 (m, 2H), 1.73–1.62 (m, 6H), 1.58–1.33 (m, 3H), 1.29–1.21 (m, 3H), 1.15–1.08 (m, 5H), 0.98–0.93 (m, 9H), 0.83 (s, 6H), 0.68 (s, 3H); ^{13}C (100 MHz, $CDCl_3$): δ 175.79, 171.07, 154.99, 134.20, 134.11, 106.87, 80.78, 63.84, 56.82, 50.36, 48.04, 47.13, 45.84, 42.70, 37.74, 36.83, 35.11, 33.64, 32.21, 30.63, 28.86, 28.17, 27.85, 26.35, 25.16, 24.05, 22.69, 21.84, 21.72, 21.34, 20.41, 19.11, 17.96, 17.35, 16.50; HRMS (ESI): calculated for $C_{71}H_{112}O_{10}Na$ $[M + Na]^+$ 1147.8147, found 1147.8113.

Procedure for the synthesis of compound A17

PA (0.09 mmol) was dissolved in THF:MeOH:H_2O (3:1:1) (5 mL). The reaction mixture was stirred at 50 °C for 5 h and then concentrated. The pH of the mixture was adjusted to 3-4 using diluted hydrochloric acid. The target compound was filtered, washed with water and dried in a vacuum.

3β,16α-dihydroxy-lanosta-8,24(31)-diene-21-oic acid (A17)

Light yellow solid; mp: 269–270 °C; yield 100%; ^{1}H (400 MHz, Pyridin-d_5): δ 4.97 (s, 1H), 4.83 (s, 1H), 4.54–4.51 (m, 1H), 3.46–3.42 (m, 1H), 2.96–2.92 (m, 1H), 2.84–2.79 (m, 1H), 2.69–2.61 (m, 1H), 2.56–2.36 (m, 4H), 2.30–1.94 (m, 7H), 1.84–1.70 (m, 4H), 1.62–1.52 (m, 2H), 1.48 (s, 3H), 1.32–1.25 (m, 1H), 1.23 (s, 3H), 1.15 (m, 3H), 1.06 (s, 3H), 1.01 (s, 3H), 0.98–0.96 (s, 6H); ^{13}C (100 MHz, Pyridin-d_5): δ 178.61, 155.79, 134.60, 134.50, 106.76, 77.72, 76.37, 57.07, 50.63, 48.54, 48.45, 45.98, 43.45, 39.28, 37.11, 35.79, 33.84, 32.98, 31.33, 29.45, 28.38, 26.70, 25.18, 21.75, 21.60, 20.70, 19.12, 18.45, 17.55, 16.14; HRMS (ESI): calculated for $C_{31}H_{50}O_4Na$ $[M + Na]^+$ 509.3601, found 509.3600.

Procedure for the synthesis of compound A18

PA(0.18 mmol) was dissolved in methanol (30 mL). Subsequently, 10% Pt/C (100 mg) was added. The mixture was stirred overnight at room temperature under a hydrogen atmosphere. The reaction was then filtered and concentrated to yield the compound **A18**.

3β-Acetoxy-16α-hydroxy-lanosta-8-ene-21-oic acid (A18)

White solid; mp: 264–266 °C; yield 100%; ^{1}H (400 MHz, Pyridin-d_5): δ 4.68 (dd, $J = 4.0$, 11.5 Hz, 1H), 4.59 (s, 1H), 2.91–2.77 (m, 2H), 2.42–1.97 (m, 10H), 1.87–1.34 (m, 16H), 1.16–1.10 (m, 5H), 0.97–0.91 (m, 9H), 0.82–0.72 (m, 9H); ^{13}C (100 MHz, Pyridin-d_5): δ 171.89, 136.31, 135.57, 81.87, 77.60, 58.65, 51.96, 49.96, 47.59, 44.76, 40.29, 39.25, 38.38, 36.67, 34.26, 33.77, 32.82, 32.10, 30.79, 29.23, 27.98, 26.82, 25.73, 22.43, 22.13, 21.72, 20.50, 19.61, 19.14, 18.58, 18.06, 16.81, 16.59; HRMS (ESI): calculated for $C_{33}H_{54}O_5Na$ $[M + Na]^+$ 553.3863, found 553.3856.

Pharmacology

Cell culture

The HepG2 and HSC-2 cell lines were purchased from Jiangsu Keygen Biotech Corp., Ltd (Nanjing, China). Two cancer cell lines were cultured in minimum essential medium (MEM) supplemented with 10% FBS at 37 °C with 5% CO_2.

Cytotoxicity effects

HepG2 and HSC-2 cells (3.5×10^4 cells/well) were seeded into 96-well plates and then incubated with 0.1% DMSO or different concentrations of test compounds with 5% CO_2 at

37 °C for 72 h. Subsequently, 10 µl CCK-8 solution was added to each well before the cells were incubated at 37 °C for 2 h. The absorbance was measured at 450 nm using a microplate reader. IC_{50} values were calculated using GraphPad Prism software (version 8.0).

Cell cycle arrest analysis

HSC-2 cells (3×10^5 cells/well) were seeded into six-well plates and incubated with 0.1% DMSO or different concentrations of test compounds with 5% CO_2 at 37 °C for 48 h. Thereafter, cells were detached using trypsin, harvested, and washed twice with PBS. The cells were fixed with ice-cold 70% ethanol at 4 °C overnight. The cells were incubated with 100 µL RNase A at 37 °C for 30 min and then with 400 µL propidium iodide at 4 °C for 30 min in the dark. The cell cycle was determined by flow cytometry.

Apoptosis analysis

HSC-2 cells (3×10^5 cells/well) were seeded into six-well plates and incubated with 0.1% DMSO or different concentrations of test compounds with 5% CO_2 at 37 °C for 48 h. The cells were trypsinized, washed twice with PBS, and collected. The cells were re-suspended in 500 µL binding buffer and stained with 5 µL Annexin V-FITC and 5 µL propidium iodide for 15 min in the dark. Subsequently, the cells were analyzed using flow cytometry.

AO/EB staining

HSC-2 cells (1×10^5 cells/well) were seeded into six-well plates and incubated with 0.1% DMSO or different concentration of test compounds with 5% CO_2 at 37 °C for 48 h. The cells were then washed twice with PBS and stained with 500 µL AO/EB dye at room temperature for 15 min in the dark. Cells were visualized under a fluorescence microscope at 100× magnification.

Western blot analysis

After culturing, HSC-2 cells (4×10^6 cells/well) were treated with 0.1% DMSO or different concentrations of test compounds with 5% CO_2 at 37 °C for 48 h. Then, the cells were harvested, washed with PBS, and lysed with cold lysis buffer, followed by centrifugation. Subsequently, the total protein was collected, and the protein concentration was quantified using the Bradford assay. Equal amounts of proteins were electrophoresed using 10% SDS-PAGE and transferred onto a nitrocellulose membrane. After blocking in 5% non-fat milk at room temperature for 2 h, the membranes were washed thrice with TBST and incubated overnight with primary antibodies at 4 °C. After washing, the membranes were incubated with HRP-conjugated secondary antibodies at room temperature for 1 h and visualized using enhanced chemiluminescence (ECL) detection kit. GADPH was used as the protein loading control.

Statistical analysis

Statistical analyses were conducted using one-way ANOVA followed by Dunnett's post-hoc test to compare the differences between groups, with $p < 0.05$ indicating significant differences. All experiments were independently performed at least thrice. Data are expressed as mean ± standard error (SD).

Funding This work was financially supported by the National Natural Science Foundation of China (grant no. 81860622), Department of Science and Technology of Zunyi City [grant no. (2020)293] and Education and Teaching Reform Program of Zunyi Medical University (grant no. ZYK38).

Compliance with ethical standards

Conflict of interest The authors declare no competing interests.

References

1. Siegel RL, Miller KD, Jemal A. Cancer statistics, 2019. CA Cancer J Clin. 2019;69:7–34. https://doi.org/10.3322/caac.21551.
2. Siegel RL, Miller KD, Jemal A. Cancer statistics, 2016. CA Cancer J Clin. 2016;66:7–30. https://doi.org/10.3322/caac.21332.
3. Robey RW, Pluchino KM, Hall MD, Fojo AT, Bates SE, Gottesman MM. Revisiting the role of ABC transporters in multidrug-resistant cancer. Nat Rev Cancer. 2018;18:452–64. https://doi.org/10.1038/s41568-018-0005-8.
4. Dallavalle S, Dobričić V, Lazzarato L, Gazzano E, Machuqueiro M, Pajeva I. et al. Improvement of conventional anti-cancer drugs as new tools against multidrug resistant tumors. Drug Resist Updat. 2020;50:100682. https://doi.org/10.1016/j.drup.2020.100682.
5. Shingu T, Tai T, Akahori A. A lanostane triterpenoid from Poria cocos. Phytochemistry. 1992;31:2548–9. https://doi.org/10.1016/0031-9422(92)83325-S.
6. Ríos JL. Chemical constituents and pharmacological properties of Poria cocos. Planta Med. 2011;77:681–91. https://doi.org/10.1055/s-0030-1270823.
7. Nie A, Chao Y, Zhang X, Jia W, Zhou Z, Zhu C. Phytochemistry and pharmacological activities of Wolfiporia cocos (F.A. Wolf) Ryvarden & Gilb. Front Pharm. 2020;11:505249. https://doi.org/10.3389/fphar.2020.505249.
8. Lai KH, Lu MC, Du YC, El-Shazly M, Wu TY, Hsu YM. et al. Cytotoxic Lanostanoids from Poria cocos. J Nat Prod. 2016;79:2805–13. https://doi.org/10.1021/acs.jnatprod.6b00575.
9. Taofiq O, Martins A, Barreiro MF, Ferreira ICFR. Anti-inflammatory potential of mushroom extracts and isolated metabolites. Trends Food Sci Tech. 2016;50:193–210. https://doi.org/10.1016/j.tifs.2016.02.005.
10. Tang X, Chen J, Shen X. The signaling pathway for regulation of glucose transporter 4 and its application in drug development. Sci Sin Chim. 2012;42:1760–73. https://doi.org/10.1360/032012-333.
11. Wu Z, Chen X, Ni W, Zhou D, Chai S, Ye W. et al. The inhibition of Mpro, the primary protease of COVID-19, by Poria cocos and

its active compounds: A network pharmacology and molecular docking study. RSC Adv. 2021;11:11821–43. https://doi.org/10.1039/d0ra07035a.
12. Pang Y, Zhu S, Pei H. Pachymic acid protects against cerebral ischemia/reperfusion injury by the PI3K/Akt signaling pathway. Metab Brain Dis. 2020;35:673–80. https://doi.org/10.1007/s11011-020-00540-3.
13. Xu H, Wang Y, Zhao J, Jurutka PW, Huang D, Liu L. et al. Triterpenes from Poria cocos are revealed as potential retinoid X receptor selective agonists based on cell and in silico evidence. Chem Biol Drug Des. 2020;95:493–502. https://doi.org/10.1111/cbdd.13610.
14. Gapter L, Wang Z, Glinski J, Ng KY. Induction of apoptosis in prostate cancer cells by pachymic acid from Poria cocos. Biochem Biophys Res Commun. 2005;332:1153–61. https://doi.org/10.1016/j.bbrc.2005.05.044.
15. Jeong JW, Lee WS, Go SI, Nagappan A, Baek JY, Lee JD. et al. Pachymic acid induces apoptosis of EJ bladder cancer cells by DR5 up-regulation, ROS generation, modulation of Bcl-2 and IAP family members. Phytother Res. 2015;29:1516–24. https://doi.org/10.1002/ptr.5402.
16. Lu C, Ma J, Cai D. Pachymic acid inhibits the tumorigenicity of gastric cancer cells by the mitochondrial pathway. Anticancer Drugs. 2017;28:170–9. https://doi.org/10.1097/CAD.0000000000000449.
17. Li G, Xu ML, Lee CS, Woo MH, Chang HW, Son JK. Cytotoxicity and DNA topoisomerases inhibitory activity of constituents from the sclerotium of Poria cocos. Arch Pharm Res. 2004;27:829–33. https://doi.org/10.1007/BF02980174.
18. Jiang Y, Fan L. Evaluation of anticancer activities of Poria cocos ethanol extract in breast cancer: In vivo and in vitro, identification and mechanism. J Ethnopharmacol. 2020;257:112851. https://doi.org/10.1016/j.jep.2020.112851.
19. Ma J, Liu J, Lu C, Cai D. Pachymic acid induces apoptosis via activating ROS-dependent JNK and ER stress pathways in lung cancer cells. Cancer Cell Int. 2015;15:78. https://doi.org/10.1186/s12935-015-0230-0.
20. Sun KX, Xia HW. Pachymic acid inhibits growth and induces cell cycle arrest and apoptosis in gastric cancer SGC-7901 cells. Oncol Lett. 2018;16:2517–24. https://doi.org/10.3892/ol.2018.8899.
21. Cheng S, Swanson K, Eliaz I, McClintick JN, Sandusky GE, Sliva D. Pachymic acid inhibits growth and induces apoptosis of pancreatic cancer in vitro and in vivo by targeting ER stress. PLoS One. 2015;10:e0122270 https://doi.org/10.1371/journal.pone.0122270.
22. Wei C, Wang H, Sun X, Bai Z, Wang J, Bai G. et al. Pharmacological profiles and therapeutic applications of pachymic acid (Review). Exp Ther Med. 2022;24:547. https://doi.org/10.3892/etm.2022.11484.
23. Wang P, She G, Yang Y, Li Q, Zhang H, Liu J. et al. Synthesis and biological evaluation of new ligustrazine derivatives as antitumor agents. Molecules. 2012;17:4972–85. https://doi.org/10.3390/molecules17054972.
24. Zhang L, Liu L, Zheng C, Wang Y, Wang J, Yao Q. Synthesis of novel indirubin derivatives and their effects on the proliferation, cell cycle and apoptosis in acute myeloblastic leukemia HL-60 cells. Chin J Org Chem. 2017;37:1523–9. https://doi.org/10.6023/cjoc201704018.
25. Wang J, Long L, Chen Y, Xu Y, Zhang L. Design, synthesis and antineoplastic activity of novel hybrids of podophyllotoxin and indirubin against human leukaemia cancer cells as multifunctional anti-MDR agents. Bioorg Med Chem Lett. 2018;28:1817–24. https://doi.org/10.1016/j.bmcl.2018.04.019.
26. Yang C, Xie Q, Zeng X, Tao N, Xu Y, Chen Y. et al. Novel hybrids of podophyllotoxin and formononetin inhibit the growth, migration and invasion of lung cancer cells. Bioorg Chem. 2019;85:445–54. https://doi.org/10.1016/j.bioorg.2019.02.019.
27. Chen X, Huang P, Wang J, Tian R, Chen Y, Chen Y. et al. Identification of H2S/NO-donating artemisinin derivatives as potential antileukemic agents. RSC Adv. 2020;10:501–11. https://doi.org/10.1039/c9ra08239e.
28. Wang H, Wang Z, Wei C, Wang J, Xu Y, Bai G. et al. Anticancer potential of indirubins in medicinal chemistry: Biological activity, structural modification, and structure-activity relationship. Eur J Med Chem. 2021;223:113652. https://doi.org/10.1016/j.ejmech.2021.113652.
29. Boechat N, da Costa JCS, de Souza Mendonça J, De Souza MVN. A simple reduction of methyl aromatic esters to alcohols using sodium borohydride–methanol system. Tetrahedron Lett. 2004;45:6021–2. https://doi.org/10.1016/j.tetlet.2004.06.034.
30. Chu BF, Lin HC, Huang XW, Huang HY, Wu CP, Kao MC. An ethanol extract of Poria cocos inhibits the proliferation of non-small cell lung cancer A549 cells via the mitochondria-mediated caspase activation pathway. J Funct Foods. 2016;23:614–27. https://doi.org/10.1016/j.jff.2016.03.016.